ELSEVIER

PII: S0965-9978(96)00027-0

Advances in Engineering Software 27 (1996) 227–238

0965-9978/95/$15.00

Dual series representation and its applications to a string subjected to support motions

J. T. Chen & Y. S. Jeng

Department of Harbor and River Engineering, Taiwan Ocean University, Keelung, Taiwan

(Received 15 August 1995; revised version received 17 October 1995; accepted 22 November 1995)

Dual series representation (DSR) for the dynamic response of a finite elastic body subjected to boundary traction and boundary support excitations is proposed in this paper. To confirm the validity of the present model, a string subjected to support motions is solved. Four analytical methods including (1) a diamond rule, (2) a series solution with the quasi-static decomposition method, (3) DSR by the Cesàro sum technique, and (4) DSR by the Stokes' transformation method are presented. It is found that the numerical results obtained by using these four methods are in good agreement, and that both the Cesàro sum and Stokes' transformation regularization techniques can extract the finite part of the divergent series. The advantages and disadvantages of these four methods are discussed. In comparison with the quasi-static decomposition method and the Cesàro sum technique, the Stokes' transformation is the best way not only because it is free from calculation of the quasi-static solution, but also because its convergence rate is as fast as that of the mode acceleration method. Copyright © 1996 Elsevier Science Limited.

Key words: dual series representation, support motions, string.

1 INTRODUCTION

Dual integral equations for degenerate boundary problems were developed in 1986[1] and have been extended to the crack problem. This numerical implementation has been termed the dual boundary element method by Portela *et al.*[8] Recently, many researchers have paid much attention to potential applications of the dual integral equations.[6,8–10] However, the applications mainly focus on the boundary value problems, and extension to initial boundary value problems has not been dealt with extensively. Traditionally, two approaches, the direct transient and the modal transient methods in the time domain, have been employed to solve initial-boundary value problems. By using the time-dependent fundamental solution, a dual integral formulation can be directly derived. However, the eigensystem for the structure considered is always known in *a priori*, either by experiment or by analysis, in engineering practice. Therefore, the modal transient method is suitable when the eigensystem is available.

In this paper, direct transient analysis by using dual integral equations (DIE) and modal transient analysis by using DSR are proposed for a finite elastic body subjected to arbitrary boundary loadings. The Cauchy singularity and hypersingularity in DIE are transformed to the Gibbs phenomenon of the series convergence in the mean and series divergence in DSR, respectively. The regularization techniques for series divergence, the Cesàro sum and Stokes' transformation, are employed to extract a finite part of an infinite value similar to the way in which the Hadamard principal value is used to obtain the finite part of the divergent integral of hypersingularity. Finally, a simple string example subjected to support motions is shown to check the validity of present modal.

2 DUAL SERIES REPRESENTATION FOR AN ELASTIC BODY SUBJECTED TO ARBITRARY LOADINGS

2.1 Problem statement

Consider a homogeneous, isotropic, linear elastic continuum with finite domain D bounded by boundary B; the governing equation for the displacement $\mathbf{u}(\mathbf{x},t)$ at a domain point $\mathbf{x}$ at time t can be written as

$$\rho\ddot{\mathbf{u}} + \mathcal{L}\{\mathbf{u}\} = 0, \mathbf{x} \in D, t \in (0,\infty), \quad (1)$$

where ρ is the mass density, and the operator $\mathcal{L}$ is

$$\mathcal{L}\{\mathbf{u}\} = \begin{cases} -(\lambda + G)\nabla\nabla \cdot \mathbf{u} - G\nabla^2\mathbf{u}, & \text{elastic body,} \\ -T\frac{\partial^2 u}{\partial x^2}, & \text{string} \end{cases} \tag{2}$$

in which λ and G are Lame's constants, and T is the tension of the string. The time-dependent boundary conditions are

$$\mathcal{T}\{\mathbf{u}(\mathbf{x},t)\} \equiv \mathbf{t}(\mathbf{x},t) = \hat{\mathbf{t}}(\mathbf{x},t), \mathbf{x} \in B_t, \tag{3}$$

$$\mathbf{u}(\mathbf{x},t) = \hat{\mathbf{u}}(\mathbf{x},t), \in B_u, \tag{4}$$

where B_t and B_u denote the specified traction and displacement boundaries, respectively, and $\hat{\mathbf{u}}$ is the prescribed displacement on B_u, $\mathbf{t}$ is the traction, $\hat{\mathbf{t}}$ is the prescribed traction on B_t, and $\mathcal{T}$ is the traction operator defined as

$$\mathcal{T}\{\mathbf{u}\} = \begin{cases} [\lambda\mathbf{I}(\nabla \cdot \mathbf{u}) + G\nabla\mathbf{u} + G\mathbf{I}\cdot(\mathbf{u}\nabla)]\cdot\mathbf{n}, & \text{elastic body,} \\ T\frac{\partial u}{\partial x}, & \text{string} \end{cases} \tag{5}$$

in which $\mathbf{n}$ is the normal vector. The initial conditions are

$$\mathbf{u}(\mathbf{x},0) = \mathbf{u}_0(\mathbf{x}), \tag{6}$$

$$\dot{\mathbf{u}}(\mathbf{x},0) = \mathbf{v}_0(\mathbf{x}). \tag{7}$$

For comparison purposes, both of the integral formulations for direct and modal transient elastodynamics are derived separately.

2.2 Direct transient elasticity

Extending the dual integral representation for boundary value problems[5,6] to transient elastodynamics, the displacement $\mathbf{u}(\mathbf{x},t)$ and traction $\mathbf{t}(\mathbf{x},t)$ for a domain point $\mathbf{x}$ at time t can be written as

$$\begin{aligned} \mathbf{u}(\mathbf{x},t) = & \int_0^t \int_B \mathbf{U}(\mathbf{s},\mathbf{x};t,\tau)\cdot\mathbf{t}(\mathbf{s},\tau)\mathrm{d}B(\mathbf{s})\mathrm{d}\tau \\ & - \int_0^t \int_B \mathbf{T}(\mathbf{s},\mathbf{x};t,\tau)\cdot\mathbf{u}(\mathbf{s},\tau)\mathrm{d}B(\mathbf{s})\mathrm{d}\tau \\ & + \int_D \mathbf{U}(\mathbf{s},\mathbf{x};t,0)\cdot\rho\mathbf{v}_0(\mathbf{s})\mathrm{d}D(\mathbf{s}) \\ & + \int_D \dot{\mathbf{U}}(\mathbf{s},\mathbf{x};t,0)\cdot\rho\mathbf{u}_0(\mathbf{s})\mathrm{d}D(\mathbf{s}), \end{aligned} \tag{8}$$

$$\begin{aligned} t,(\mathbf{x},t) = & \int_0^t \int_B \mathbf{L}(\mathbf{s},\mathbf{x};t,\tau)\cdot\mathbf{t}(\mathbf{s},\tau)\mathrm{d}B(\mathbf{s})\mathrm{d}\tau \\ & - \int_0^t \int_B \mathbf{M}(\mathbf{s},\mathbf{x};t,\tau)\cdot\mathbf{u}(\mathbf{s},\tau)\mathrm{d}B(\mathbf{s})\mathrm{d}\tau \\ & + \int_D \mathbf{L}(\mathbf{s},\mathbf{x};t,0)\cdot\rho\mathbf{v}_0(\mathbf{s})\mathrm{d}D(\mathbf{s}) \\ & + \int_D \dot{\mathbf{L}}(\mathbf{s},\mathbf{x};t,0)\cdot\rho\mathbf{u}_0(\mathbf{s})\mathrm{d}D(\mathbf{s}), \end{aligned} \tag{9}$$

where $\mathbf{U}(\mathbf{s},\mathbf{x};t,\tau)$, $\mathbf{T}(\mathbf{s},\mathbf{x};t,\tau)$, $\mathbf{L}(\mathbf{s},\mathbf{x};t,\tau)$ and $\mathbf{M}(\mathbf{s},\mathbf{x};t,\tau)$ are four kernel functions. The closed-form solutions can be found in Ref. 6. The dual integral formulations for the displacement and traction on a boundary point $\mathbf{x}$ at time t are

$$\begin{aligned} c\mathbf{u}(\mathbf{x},t) = & R.P.V. \int_0^t \int_B \mathbf{U}(\mathbf{s},\mathbf{x};t,\tau)\cdot\mathbf{t}(\mathbf{s},\tau)\mathrm{d}B(\mathbf{s})\mathrm{d}\tau \\ & - C.P.V. \int_0^t \int_B \mathbf{T}(\mathbf{s},\mathbf{x};t,\tau)\cdot\mathbf{u}(\mathbf{s},\tau)\mathrm{d}B(\mathbf{s})\mathrm{d}\tau \\ & + \int_D \mathbf{U}(\mathbf{s},\mathbf{x};t,0)\cdot\rho\mathbf{v}_0(\mathbf{s})\mathrm{d}D(\mathbf{s}) \\ & + \int_D \dot{\mathbf{U}}(\mathbf{s},\mathbf{x};t,0)\cdot\rho\mathbf{u}_0(\mathbf{s})\mathrm{d}D(\mathbf{s}), \end{aligned} \tag{10}$$

$$\begin{aligned} c\mathbf{t}(\mathbf{x},t) = & C.P.V. \int_0^t \int_B \mathbf{L}(\mathbf{s},\mathbf{x};t,\tau)\cdot\mathbf{t}(\mathbf{s},\tau)\mathrm{d}B(\mathbf{s})\mathrm{d}\tau \\ & - H.P.V. \int_0^t \int_B \mathbf{M}(\mathbf{s},\mathbf{x};t,\tau)\cdot\mathbf{u}(\mathbf{s},\tau)\mathrm{d}B(\mathbf{s})\mathrm{d}\tau \\ & + \int_D \mathbf{L}(\mathbf{s},\mathbf{x};t,0)\cdot\rho\mathbf{v}_0(\mathbf{s})\mathrm{d}D(\mathbf{s}) \\ & + \int_D \dot{\mathbf{L}}(\mathbf{s},\mathbf{x};t,0)\cdot\rho\mathbf{u}_0(\mathbf{s})\mathrm{d}D(\mathbf{s}), \end{aligned} \tag{11}$$

where c is 1/2 for 1-D, π for 2-D, or 2π for 3-D on a smooth boundary, and $R.P.V.$, $C.P.V.$ and $H.P.V.$ denote the Rieman integral, the Cauchy principal value and the Hadamard (or Mangler) principal value, respectively. In discretized numerical calculations, it is found that matrix inversion is necessary at each time-marching stage for the direct transient method. To avoid these repetitive time-consuming inversions, the modal transient method is employed in the following.

Modal transient elasticity

In the derivation procedure, let the solution be decomposed into two parts:[11]

$$\mathbf{u}(\mathbf{x},t) = \mathbf{U}(\mathbf{x},t) + \sum_{k=1}^{\infty} q_k(t)\mathbf{u}_k(\mathbf{x}), \tag{12}$$

where $\mathbf{U}(\mathbf{x},t)$ denotes the quasi-static solution. The second term, which is composed of various eigenfunctions $\mathbf{u}_k(\mathbf{x})$, ($k \in N$, N denotes the set of natural numbers), and is weighted by generalized coordinates $q_k(t)$, is the dynamic contribution due to the inertia effect. Following the same procedures in Ref. 13 the displacement $\mathbf{u}(\mathbf{x},t)$ can be represented by introducing a more generalized coordinate, $\bar{q}_k(t)$, as in the following series:

$$\mathbf{u}(\mathbf{x},t) = \sum_{k=1}^{\infty} \bar{q}_k(t)\mathbf{u}_k(\mathbf{x})$$

$$= \sum_{m=1}^{\infty}\left\{\frac{\lambda_m}{N_m}\cos(\omega_m t) + \frac{\kappa_m}{\omega_m N_m}\sin(\omega_m t) + \frac{1}{\omega_m N_m}\int_0^t [U_m^B(\tau) - T_m^B(\tau)] \sin(\omega_m(t-\tau))\mathrm{d}\tau\right\}\mathbf{u}_m(\mathbf{x}) \quad (13)$$

where

$$\int_D \rho\mathbf{u}_m(\mathbf{x})\cdot\mathbf{u}_n(x)\mathrm{d}D(x) = \begin{cases} 0, \text{if } n \neq m \\ N_m, \text{if } n = m \end{cases} \quad (14)$$

$$\lambda_m \equiv \int_D \rho\mathbf{u}_0(\mathbf{x})\cdot\mathbf{u}_m(\mathbf{x})\mathrm{d}D(\mathbf{x}), \quad (15)$$

$$\kappa_m \equiv \int_D \rho\mathbf{v}_0(\mathbf{x})\cdot\mathbf{u}_m(\mathbf{x})\mathrm{d}D(\mathbf{x}), \quad (16)$$

$$U_m^B(t) \equiv \int_B \mathbf{u}_m(\mathbf{s})\cdot\hat{\mathbf{t}}(\mathbf{s},t)\mathrm{d}B(\mathbf{s}) \quad (17)$$

$$T_m^B(t) \equiv \int_{B_u} \mathbf{t}_m(\mathbf{s})\cdot\hat{\mathbf{u}}(\mathbf{s},t)\mathrm{d}B(\mathbf{s}), \quad (18)$$

in which D is the considered domain, ω_m is the mth modal frequency, and $\mathbf{t}_m(\mathbf{x})$ is the mth modal reaction. Without thoughtful consideration, we apply a traction operator to the summation sign of eqn (13) to obtain

$$\mathbf{t}(\mathbf{x},t) = \sum_{m=1}^{\infty}\left\{\frac{\lambda_m}{N_m}\cos(\omega_m t) + \frac{\kappa_m}{\omega_m N_m}\sin(\omega_m t) + \frac{1}{\omega_m N_m}\int_0^t [U_m^B(\tau) - T_m^B(\tau)] \sin(\omega_m(t-\tau))\mathrm{d}\tau\right\}\mathbf{t}_m(\mathbf{x}). \quad (19)$$

Comparing eqns (13) and (19) with eqns (8) and (9), we have

$$\mathbf{U}(\mathbf{s},\mathbf{x};t,\tau) = \sum_{m=1}^{\infty}\frac{1}{N_m\omega_m}\sin(\omega_m(t-\tau))\mathbf{u}_m(\mathbf{x})\otimes\mathbf{u}_m(\mathbf{s}), \quad (20)$$

$$\mathbf{T}(\mathbf{s},\mathbf{x};t,\tau) = \sum_{m=1}^{\infty}\frac{1}{N_m\omega_m}\sin(\omega_m(t-\tau))\mathbf{u}_m(\mathbf{x})\otimes\mathbf{t}_m(\mathbf{s}), \quad (21)$$

$$\mathbf{L}(\mathbf{s},\mathbf{x};t,\tau) = \sum_{m=1}^{\infty}\frac{1}{N_m\omega_m}\sin(\omega_m(t-\tau))\mathbf{t}_m(\mathbf{x})\otimes\mathbf{u}_m(\mathbf{s}), \quad (22)$$

$$\mathbf{M}(\mathbf{s},\mathbf{x};t,\tau) = \sum_{m=1}^{\infty}\frac{1}{N_m\omega_m}\sin(\omega_m(t-\tau))\mathbf{t}_m(\mathbf{x})\otimes\mathbf{t}_m(\mathbf{s}), \quad (23)$$

where $\otimes$ is the dyadic product. Equations (20)–(23) can be seen as the spectral decomposition for closed-form kernels in eqns (8) and (9). Therefore, the strong singularity in eqn (10) and hypersingularity in eqn (10) in DIE are changed to series convergence in the mean with Gibbs phenomenon and series divergence, respectively. In order to accelerate the convergence rate to deal with the Gibbs phenomenon, the Cesàro sum of order $(C, 1)$ is applied to eqn (13) while the $(C, 2)$ operator is utilized to extract the finite part of the divergent series of eqn (19) as follows:

$$\mathbf{u}(\mathbf{x},t) = (C,1)\left\{\sum_{m=1}^{k}\left\{\frac{\lambda_m}{N_m}\cos(\omega_m t) + \frac{\kappa_m}{\omega_m N_m}\sin(\omega_m t) + \frac{1}{\omega_m N_m}\int_0^t [U_m^B(\tau) - T_m^B(\tau)] \sin(\omega_m(t-\tau))\mathrm{d}\tau\right\}\mathbf{u}_m(\mathbf{x})\right\}. \quad (24)$$

$$\mathbf{t}(\mathbf{x},t) = (C,2)\left\{\sum_{m=1}^{k}\left\{\frac{\lambda_m}{N_m}\cos(\omega_m t) + \frac{\kappa_m}{\omega_m N_m}\sin(\omega_m t) + \frac{1}{\omega_m N_m}\int_0^t [U_m^B(\tau) - T_m^B(\tau)] \sin(\omega_m(t-\tau))\mathrm{d}\tau\right\}\mathbf{t}_m(\mathbf{x})\right\}, \quad (25)$$

where $(C, 1)$ and $(C, 2)$ are defined by Ref. 12

$$(C,1)\left\{\sum_{n=0}^{k} a_n\right\} \equiv \frac{1}{k+1}\sum_{n=0}^{k}(k-n+1)a_n \quad (26)$$

$$(C,2)\left\{\sum_{n=0}^{k} a_n\right\} \equiv \frac{1}{(k+1)(k+2)} \sum_{n=0}^{k}(k-n+1)(k-n+2)a_n, \quad (27)$$

and finite k terms are considered in real calculations. If regularized, eqns (24) and (25) are the dual integral representation in series form or, for brevity, the dual series representation.[12] Each term of the series is seen to be a general *Duhamel* integral. Its kernel functions $\mathbf{U}(\mathbf{s},\mathbf{x};t,\tau)$, $\mathbf{T}(\mathbf{s},\mathbf{x};t,\tau)$, $\mathbf{L}(\mathbf{s},\mathbf{x};t,\tau)$, and $\mathbf{M}(\mathbf{s},\mathbf{x};t,\tau)$ all have the same oscillating factor sin $(\omega_m(t-\tau))$ and represent system characteristics whereas its density functions represent input excitations, but the initial disturbances appear in the free terms, λ_m and κ_m, outside the integral signs.

3 REGULARIZATION BY THE STOKES' TRANSFORMATION

Stokes' theorem has been employed[15] to treat the hypersingularity. Since the DIE is transformed to DSR, the termwise differentiation in DSR results in divergent series in a similar way that hypersingularity occurs in the differentiation of singular boundary integral. Stokes' transformation can extract the finite part of the divergent series. From the standpoint of ordinary convergence in Fourier series, the legitimacy of term by term differentiation of series can only be guaranteed by rather strong requirements. We shall relax this constraint by using the regularization techniques of Stokes' transformation instead of a posterior treatment of the Cesàro sum, which has been discussed in the previous section and in detail in Refs 12 and 14.

3.1 One-dimensional case of second order operator $\partial^2/\partial x^2$ for a string

A string subjected to support motions is considered in this subsection. The series representation for the displacement can be written as

$$u(x,t)=\sum_{n=1}^{\infty}\bar{q}_n(t)u_n(x), \quad 0<x<l, \tag{28}$$

where l is the length of the string, $\bar{q}_n(t)$ is the generalized coordinate, and $u_n(x)$ is the modal shape with the following properties:

$$\int_p^l u_m(x)u_n(x)\mathrm{d}x=\begin{cases}0, & \text{if } n\neq m\\ N_m, & \text{if } n=m\end{cases} \tag{29}$$

$$\bar{q}_n(t)=\frac{1}{N_n}\int_0^n u(x,t)u_n(x)\mathrm{d}x. \tag{30}$$

The series differentiation by Stokes' transformation shows

$$u'(x,t)=\sum_{n=1}^{\infty}\bar{q}'_n(t)u'_n(x), \quad 0\leq x\leq l, \tag{31}$$

where

$$\bar{q}'_n(t)=\frac{1}{N_n\lambda_n}\{u(y,t)u'_n(y)\}\Big|_{y=0}^{y=l}+\bar{q}_n(t), \tag{32}$$

$$\int_0^l u'_m(x)u'_n(x)\mathrm{d}x=\begin{cases}0, & \text{if } n\neq m\\ N_m\lambda_m, & \text{if } n=m\end{cases} \tag{33}$$

$$u''_n(x)=-\lambda_n u_n(x). \tag{34}$$

Therefore,

$$u'(x,t)=\sum_{n=1}^{\infty}\frac{1}{N_n\lambda_n}\{u(y,t)u'_n(y)\}\Big|_{y=0}^{y=l}u'_n(x)+\sum_{n=1}^{\infty}\bar{q}_n(t)u'_n(x), \quad 0\leq x\leq l. \tag{35}$$

In eqn (35), it is easily found that the term by term differentiation drives away the boundary terms $1/N_n\lambda_n\{u(y,t)u'_n(y)\}|y=1/y=0u'_n(x)$ and causes the series to diverge. The Stokes' transformation method causes the series to converge by including the boundary term.

3.2 Navier operator for dynamic elasticity

The representation of the displacement field for a finite elastic body can be expressed in component form:

$$u_i(\mathbf{x},t)=\sum_{n=1}^{\infty}\bar{q}_n(t)u_i^n(\mathbf{x}), \tag{36}$$

where

$$\delta_{mn}=\int_D u_i^m(\mathbf{x})u_i^n(\mathbf{x})\mathrm{d}D \tag{37}$$

$$\bar{q}_n(t)=\int_D u_i(\mathbf{x},t)u_i^n(\mathbf{x})\mathrm{d}D, \tag{38}$$

where the subscript of $u_i^n(\mathbf{x})$ indicates the ith component of displacement, and the superscript denotes the nth mode. First of all, we define the Navier operator:

$$\mathcal{D}_{ij}\equiv(\lambda+G)\partial_i\partial_j+G\delta_{ij}\delta_k\delta_k. \tag{39}$$

Applying the Navier operator to u_j, we have

$$D_{ij}u_j=(\lambda+G)u_{j,ij}+Gu_{i,kk}=\sigma_{ij,j}. \tag{40}$$

The strain field is

$$\epsilon_{ij}=\frac{1}{2}(u_{i,j}+u_{j,i}), \tag{41}$$

and the stress field is

$$\sigma_{ij}=\lambda\epsilon_{kk}\delta_{ij}+2G\epsilon_{ij}=\lambda u_{k,k}\delta_{ij}+G(u_{i,j}+u_{j,i}). \tag{42}$$

The above equation can be written in terms of the $\mathcal{D}_{ijk}^{\sigma}$ operator:

$$\sigma_{ij}=\lambda\delta_{ij}\partial_k u_k+G(\partial_j\delta_{ik}+\partial_i\delta_{jk})u_k=\mathcal{D}_{ijk}^{\sigma}u_k, \tag{43}$$

where the $\mathcal{D}_{ijk}^{\sigma}$ operator is

$$\mathcal{D}_{ijk}^{\sigma}\equiv\lambda\delta_{ij}\partial_k+G(\partial_j\delta_{ik}+\partial_i\delta_{jk}). \tag{44}$$

Comparing eqns (40) and (44), the relation between the $\mathcal{D}_{ijk}^{\sigma}$ and $\mathcal{D}_{ij}$ operators is

$$\partial_j\mathcal{D}_{ijk}^{\sigma}=\mathcal{D}_{ik}. \tag{45}$$

Changing k and j in eqn (44), we have

$$\mathcal{D}_{ijk}^{\sigma}\equiv\lambda\delta_{ik}\partial_j+G(\partial_k\delta_{ij}+\partial_i\delta_{kj}). \tag{46}$$

Define the traction operator $\mathcal{B}_{ij}$ as

$$\mathcal{B}_{ij} \equiv \mathcal{D}^{\sigma}_{ikj} n_k \equiv \lambda n_i \partial_j + G(\delta_{ij} n_k \partial_k + n_j \partial_i). \tag{47}$$

Field representation of stress can be written as

$$\sigma_{ik} = \mathcal{D}^{\sigma}_{ikj} u_j = \sum_{n=1}^{\infty} \bar{q}^{\sigma}_n(t) \mathcal{D}^{\sigma}_{ikj} u^n_j = \sum_{n=1}^{\infty} \bar{q}^{\sigma}_n(t) \sigma^n_{ik}, \tag{48}$$

where

$$\bar{q}^{\sigma}_p(t) = \frac{1}{\lambda_p}\left\{\int_D u^p_{i,k} \mathcal{D}^{\sigma}_{ikj} u_j \mathrm{d}D\right\}, \tag{49}$$

in which

$$\int_D \mathcal{D}^{\sigma}_{ikj} u^m_j u^n_{i,k} \mathrm{d}D = \begin{cases} 0, & \text{if } n \neq m \\ \lambda_m, & \text{if } n = m \end{cases} \tag{50}$$

$$\mathcal{D}_{ij} u^n_j(\mathbf{x}) = -\lambda_n u^n_i(\mathbf{x}), \tag{51}$$

where λ_n is an eigenvalue. After using

$$\begin{aligned}\int_B u^n_i \mathcal{B}_{ij} u^p_j \mathrm{d}B &= \int_B u^n_i \mathcal{D}^{\sigma}_{ikj} u^p_j n_k \mathrm{d}B \\ &= \int_D \partial_k \{u^n_i \mathcal{D}^{\sigma}_{ikj} u^p_j\} \mathrm{d}D \\ &= \int_D u^n_{i,k} \mathcal{D}^{\sigma}_{ikj} u^p_j \mathrm{d}D \\ &\quad + \int_D u^n_i \partial_k \{\mathcal{D}^{\sigma}_{ikj} u^p_j\} \mathrm{d}D,\end{aligned} \tag{52}$$

changing n and p, and using Betti's law, we have

$$\int_D u^n_{i,k} \mathcal{D}^{\sigma}_{ikj} u^p_j \mathrm{d}D = \int_D u^p_{i,k} \mathcal{D}^{\sigma}_{ikj} u^n_j \mathrm{d}D. \tag{53}$$

Using eqn (53), eqn (49) can be rewritten as

$$\begin{aligned}\bar{q}^{\alpha}_p(t) &= \frac{1}{\lambda_p}\left\{\int_D u^p_{i,k} \mathcal{D}^{\sigma}_{ikj} u_j \mathrm{d}D\right\} \\ &= \frac{1}{\lambda_p}\left\{\int_{B_u} u_i t^p_i \mathrm{d}B\right\} + \bar{q}_p(t).\end{aligned} \tag{54}$$

Therefore, the traction field can be represented by

$$t_i(\mathbf{x}) = \sum_{n=1}^{\infty} \bar{q}^{\alpha}_n(t) t^n_i(\mathbf{x}). \tag{55}$$

Substituting eqn (54) into eqn (55), we have

$$t_i(\mathbf{x}) = \sum_{n=1}^{\infty} \frac{1}{\lambda_n}\left\{\int_{B_u} u_i t^n_i \mathrm{d}B\right\} t^n_i(\mathbf{x}) + \sum_{n=1}^{\infty} \bar{q}_n(t) t^n_i(\mathbf{x}). \tag{56}$$

Equation (56) also reveals that the term by term traction derivative of eqn (36) loses the boundary terms $\sum_{n=1}^{\infty} 1/\lambda_n \{\int_{B_u} u t^n_i \mathrm{d}B\} t^n_i(\mathbf{x})$ on the right-hand side of the equals sign in eqn (56) and makes the series diverge.

After the secondary fields (stress/traction) are determined, the primary field (displacement) can be easily integrated, and the essential time-dependent boundary condition, i.e. the support motions, can be automatically included.

4 REDUCTION TO A STRING SUBJECTED TO SUPPORT MOTIONS

To check the validity of the proposed model, the string problem subjected to support motions is illustrated. The governing equation can be reduced to

$$\ddot{u} = c^2 u_{xx}, \quad \text{for } 0 < x < l,\ t > 0, \tag{57}$$

with initial conditions

$$u(x, 0) = 0 \tag{58}$$

$$\dot{u}(x, 0) = 0 \tag{59}$$

and boundary conditions

$$u(0, t) = a(t) \tag{60}$$

$$u(l, t) = b(t), \tag{61}$$

where $a(t)$ and $b(t)$ are support motions.

According to eqns (20)–(23), the four kernel functions can be decomposed as follows:

$$U(s, x; t, \tau) = \sum_{n=1}^{\infty} \frac{2}{cn\pi} \sin\left(\frac{cn\pi}{l}(t-\tau)\right) \sin\left(\frac{n\pi x}{l}\right) \sin\left(\frac{n\pi s}{l}\right) \tag{62}$$

$$T(s, x; t, \tau) = \sum_{n=1}^{\infty} \frac{2}{lc} \sin\left(\frac{cn\pi}{l}(t-\tau)\right) \sin\left(\frac{n\pi x}{l}\right) \cos\left(\frac{n\pi s}{l}\right) \tag{63}$$

$$L(s, x; t, \tau) = \sum_{n=1}^{\infty} \frac{2}{lc} \sin\left(\frac{cn\pi}{l}(t-\tau)\right) \cos\left(\frac{n\pi x}{l}\right) \sin\left(\frac{n\pi s}{l}\right) \tag{64}$$

$$M(s, x; t, \tau) = \sum_{n=1}^{\infty} \frac{2n\pi}{(l^2 c)} \sin\left(\frac{cn\pi}{l}(t-\tau)\right) \cos\left(\frac{n\pi x}{l}\right) \cos\left(\frac{n\pi s}{l}\right), \tag{65}$$

where the fundamental solution, $U(x, s; t, \tau)$, satisfies

$$\frac{1}{c^2}\ddot{U}(x, s; t, \tau) - \frac{\partial^2 U(x, s; t, \tau)}{\partial x^2} = \delta(x-s)\delta(t-\tau), \quad -\infty < x < \infty, t > 0. \tag{66}$$

Based on the dual representation model, the displacement of $u(x, t)$ is derived as

$$\begin{aligned}\mathbf{u}(\mathbf{x}, t) &= c^2 \int_0^t \int_B \mathbf{U}(\mathbf{s}, \mathbf{x}; t, \tau) \cdot \mathbf{t}(s, \tau) \mathrm{d}B(s) \mathrm{d}\tau \\ &\quad - \int_0^t \int_B \mathbf{T}(\mathbf{s}, \mathbf{x}; t, \tau) \cdot \mathbf{u}(\mathbf{s}, \tau) \mathrm{d}B(\mathbf{s}) \mathrm{d}\tau, \\ &= -c^2 \int_0^t \mathbf{T}(\mathbf{s}, \mathbf{x}; t, \tau) \cdot \mathbf{u}(\mathbf{s}, \tau) \Big|_{s=0}^{s=l} \mathrm{d}\tau.\end{aligned} \tag{67}$$

The slope of $u'(x,t)$ is derived as

$$\mathbf{t}(\mathbf{x},t) = c^2 \int_0^t \int_B \mathbf{L}(\mathbf{s},\mathbf{x};t,\tau)\cdot\mathbf{t}(\mathbf{s},\tau)\mathrm{d}B(\mathbf{s})\mathrm{d}\tau - \int_0^t \int_B \mathbf{M}(\mathbf{s},\mathbf{x};t,\tau)\cdot\mathbf{u}(\mathbf{s},\tau)\mathrm{d}B(\mathbf{s})\mathrm{d}\tau = -c^2 \int_0^t \mathbf{M}(\mathbf{s},\mathbf{x};t,\tau)\cdot\mathbf{u}(\mathbf{s},\tau)\Big|_{s=0}^{s=l}\mathrm{d}\tau, \tag{68}$$

since only B_u is present as eqns (60) and (61) show.

4.1 Diamond rule

For such a simple problem, the analytical solution by using the method of characteristics, or the so-called diamond rule, is obtained as follows:

$$u_{\mathrm{I}}(x,t) = 0 \tag{69}$$

$$u_{\mathrm{II}}(x,t) = b\left(\frac{x+ct-l}{c}\right) \tag{70}$$

$$u_{\mathrm{III}}(x,t) = a\left(\frac{ct-x}{c}\right) \tag{71}$$

$$u_{\mathrm{VI}}(x,t) = b\left(\frac{x+ct-l}{c}\right) + a\left(\frac{ct-x}{c}\right), \tag{72}$$

where the subscripts I, II, III and IV denote the regions in the (x,t) plane as shown in Fig. 1. Since no information arrives in region I, we have

$$u_{\mathrm{I}}(x,t) = 0 \tag{73}$$

For the solution in the central region as shown in Fig. 1, we have

$$U(i) = u_1 + \sum_{n=2}^{i} u_n, \tag{74}$$

where

$$u_n = \begin{cases} a(t - \frac{x}{c} - \frac{(2m-2)l}{c}) + b(t + \frac{x}{c} - \frac{(2m-1)l}{c}), & n = 2m \\ -a(t + \frac{x}{c} - \frac{2ml}{c}) - b(t - \frac{x}{c} - \frac{(2m-1)l}{c}), & n = 2m+1 \end{cases} \tag{75}$$

For the solution in the left region, we have

$$L(i) = U(i) + D, \tag{76}$$

where

$$D = \begin{cases} a(t - \frac{x+(2m-2)l}{c}), & n = 2m-1 \\ -b(t - \frac{x(2m-1)l}{c}), & n = 2m. \end{cases} \tag{77}$$

For the solution in the right region, we have

$$R(i) = U(i) + D \tag{78}$$

where

$$D = \begin{cases} b(t + \frac{x-(2m-1)l}{c}), & n = 2m-1 \\ -a(t + \frac{x-2ml}{c}), & n = 2m. \end{cases} \tag{79}$$

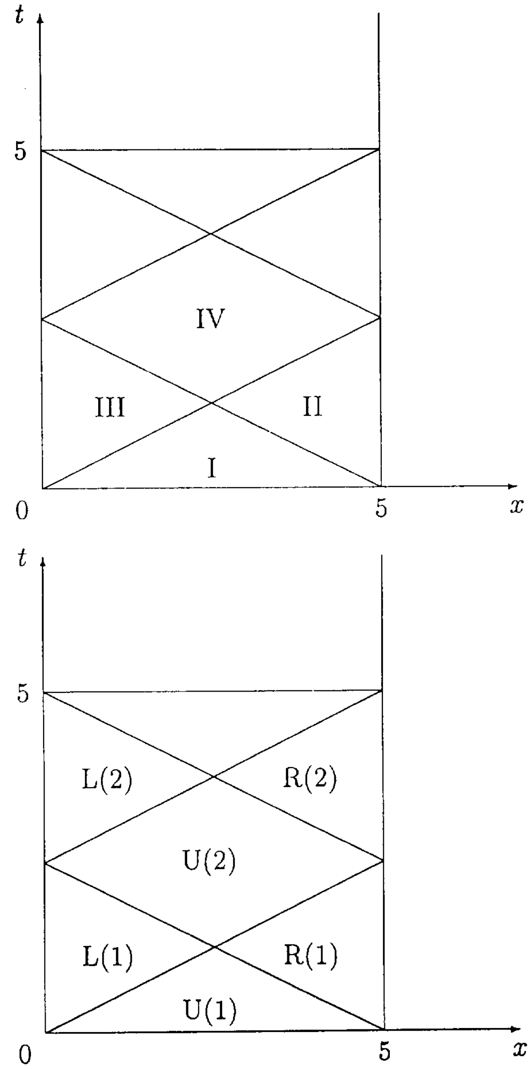

Fig. 1. Diamond rule solution for each region.

4.2 Eigenfunction expansion

By assuming the solution to be in series form, we have

$$u(x,t) = \sum_{n=1}^{\infty}\left(\frac{2c}{l}\int_0^t (a(\tau) - b(\tau)(-1)^n) \sin\frac{cnt}{l}(t-\tau)\mathrm{d}\tau\right)\sin\left(\frac{n\pi x}{l}\right) \tag{80}$$

$$u'(x,t) = \sum_{n=1}^{\infty}\left(\frac{2c}{l}\int_0^t (a(\tau) - b(\tau)(-1)^n) \sin\frac{cnt}{l}(t-\tau)\mathrm{d}\tau\right)\frac{n\pi}{l}\cos\left(\frac{n\pi x}{l}\right). \tag{81}$$

However, $u(x,t)$ presents the Gibbs phenomenon, and $u'(x,t)$ results in a divergent series. Therefore, regularization techniques are used to represent the solutions more efficiently in the following subsections.

4.3 Series solution regularized by the Cesàro sum

If eqns (80) and (81) are regularized with the Cesàro sum, we have

$$u(x,t) = (C,1)\sum_{n=1}^{\infty}\Big(\frac{2c}{l}\int_0^t (a(\tau) - b(\tau)(-1)^n) \sin\frac{cnt}{l}(t-\tau)\mathrm{d}\tau\Big)\sin\Big(\frac{n\pi x}{l}\Big) \quad (82)$$

$$u'(x,t) = (C,2)\sum_{n=1}^{\infty}\Big(\frac{2c}{l}\int_0^t (a(\tau) - b(\tau)(-1)^n) \sin\frac{cnt}{l}(t-\tau)\mathrm{d}\tau\Big)\frac{n\pi}{l}\cos\Big(\frac{n\pi x}{l}\Big). \quad (83)$$

4.4 Series solution regularized by the Stokes' transformation

By employing the Stokes' transformation, we have

$$u'(x,t) = \sum_{n=1}^{\infty}\Big\{\frac{2}{n\pi}(b(t)(-1)^n - a(t)) + \frac{2c}{l}\int_0^t (a(\tau) - b(\tau)(-1)^n) \sin\frac{cn\pi}{l}(t-\tau)\mathrm{d}\tau\Big\}\frac{n\pi}{l}\cos\Big(\frac{n\pi x}{l}\Big). \quad (84)$$

Equation (84) of the Stokes' transformation method differs from eqn (81) of the eigenfunction expansion method with a boundary term $2/n\pi(b(t)(-1)^n - a(t))$, which can cause a divergent series to converge. After integrating the slope with respect to x, we have the displacement solution:

$$u(x,t) = \sum_{n=1}^{\infty}\Big\{\frac{2}{n\pi}(b(t)(-1)^n 1 - a(t)) + \frac{2c}{l}\int_0^t (a(\tau) - b(\tau)(-1)^n) \sin\frac{cn\pi}{l}(t-\tau)\mathrm{d}\tau\Big\}\sin\Big(\frac{n\pi x}{l}\Big) + a(t). \quad (85)$$

It is easily found that the essential time-dependent boundary condition is automatically included in eqn (85), which has two more terms than does eqn (80).

4.5 Series solution by using the quasi-static decomposition method

By decomposing the quasi-static part first, we have

$$u(x,t) = \sum_{n=1}^{\infty}\Big(\frac{2l}{cn^2\pi^2}\sin\Big(\frac{cn\pi}{l}t\Big)(b'(0)(-1)^n - a'(0)) + \frac{2}{n\pi}(b(0)(-1)^n - a(0))\cos\Big(\frac{cn\pi}{l}t\Big) + \frac{2l}{cn^2\pi^2}\int_0^t \sin\Big(\frac{cn\pi}{l}(t-\tau)\Big)(b''(\tau)(-1)^n - a''(\tau))\mathrm{d}\tau\Big)\sin\Big(\frac{n\pi x}{l}\Big) + a(t)\Big(1-\frac{x}{l}\Big) + b(t)\frac{x}{l}. \quad (86)$$

Since the above series converges uniformly, termwise differentiation is permissible to obtain the following slope field:

$$u'(x,t) = \sum_{n=1}^{\infty}\Big(\frac{2l}{cn^2\pi^2}\sin\Big(\frac{cn\pi}{l}t\Big)(b'(0)(-1)^n - a'(0)) + \frac{2}{n\pi}(b(0)(-1)^n 1 - a(0))\cos\Big(\frac{cn\pi}{l}t\Big) + \frac{2l}{cn^2\pi^2}\int_0^t \sin\Big(\frac{cn\pi}{l}(t-\tau)\Big)(b''(\tau)(-1)^n - a''(\tau))\mathrm{d}\tau\Big)\Big(\frac{n\pi}{l}\Big)\cos\Big(\frac{n\pi x}{l}\Big) - a(t)\frac{1}{l} + b(t)\frac{1}{l}. \quad (87)$$

5 RESULTS AND DISCUSSION

By setting

$$l = 5, c = 2, a(t) = b(t) = \sin(t),$$

the above solutions can be obtained as shown below.

5.1 Diamond rule

In the space–time region of $(0 < x < 5, 0 < t < 5)$, the solution of the diamond rule is

$$u_{\mathrm{I}}(x,t) = 0 \quad (88)$$

$$u_{\mathrm{II}}(x,t) = \sin\Big(\frac{x+ct-l}{c}\Big) \quad (89)$$

$$u_{\mathrm{III}}(x,t) = \sin\Big(\frac{ct-x}{c}\Big) \quad (90)$$

$$u_{\mathrm{VI}}(x,t) = \sin\Big(\frac{x+ct-l}{c}\Big) + \sin\Big(\frac{ct-x}{c}\Big). \quad (91)$$

5.2 Eigenfunction expansion

By substituting l, c and $\sin(t)$ into eqns (80) and (81), we have

$$u(x,t) = \sum_{n=1}^{\infty}\left[\frac{-2cl(1-(-1)^n)}{(c^2n^2\pi^2-l^2)}\sin(n\pi ct/l) + \frac{2n\pi c^2(1-(-1)^n)}{(c^2n^2\pi^2-l^2)}\sin(t)\right]\sin(n\pi x/l) \quad (92)$$

$$u'(x,t) = \sum_{n=1}^{\infty}\left[\frac{-2cl(1-(-1)^n)\sin(n\pi ct/l)}{(c^2n^2\pi^2-l^2)} + \frac{2n\pi c^2(1-(-1)^n)\sin(t)}{(c^2n^2\pi^2-l^2)}\right](n\pi/l)\cos(n\pi x/l) \quad (93)$$

5.3 Series solution regularized by using the Cesàro sum technique

By substituting l, c and $\sin(t)$ into eqns (82) and (83), we have

$$u(x,t) = (C,1)\sum_{n=1}^{\infty}\left[\frac{-2cl(1-(-1)^n)}{c^2n^2\pi^2-l^2}\sin\left(\frac{n\pi ct}{l}\right) + \frac{2n\pi c^2(1-(-1)^n)}{c^2n^2\pi^2-l^2}\sin(t)\right]\sin\left(\frac{n\pi x}{l}\right) \quad (94)$$

$$u'(x,t) = (C,2)\sum_{n=1}^{\infty}\left[\frac{-2cl(1-(-1)^n)}{c^2n^2\pi^2-l^2}\sin\left(\frac{n\pi ct}{l}\right) + \frac{2n\pi c^2(1-(-1)^n)}{c^2n^2\pi^2-l^2}\sin(t)\right]\frac{n\pi}{l}\cos\left(\frac{n\pi x}{l}\right). \quad (95)$$

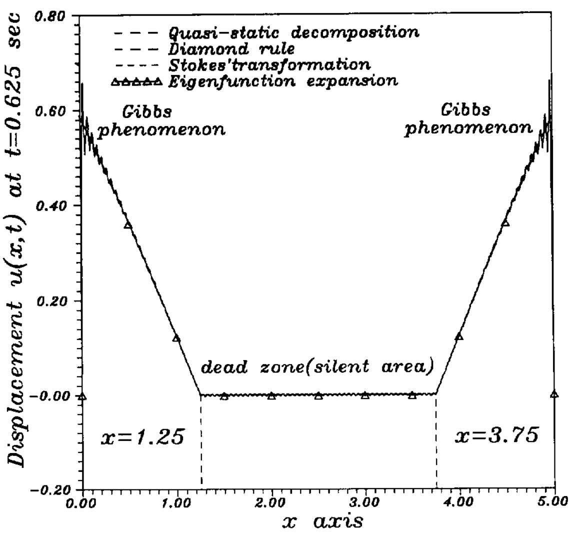

Fig. 2. Displacement profiles at $t = 0{\cdot}625$ s using the diamond rule, eigenfunction expansion, quasi-static decomposition and Stokes' transformation.

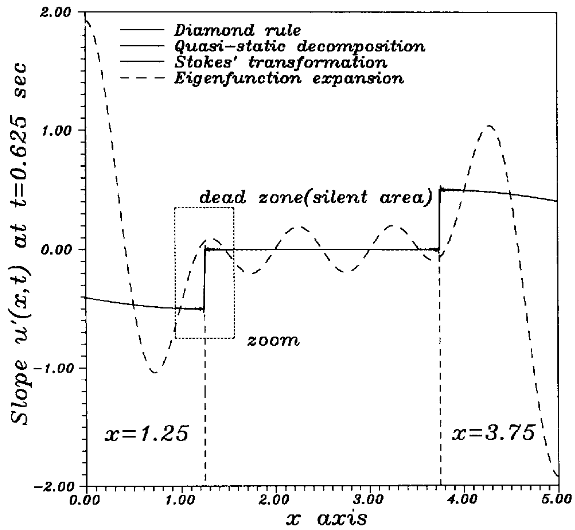

Fig. 3. Slope profiles at $t = 0{\cdot}625$ s using the diamond rule, eigenfunction expansion, quasi-static decomposition and Stokes' transformation.

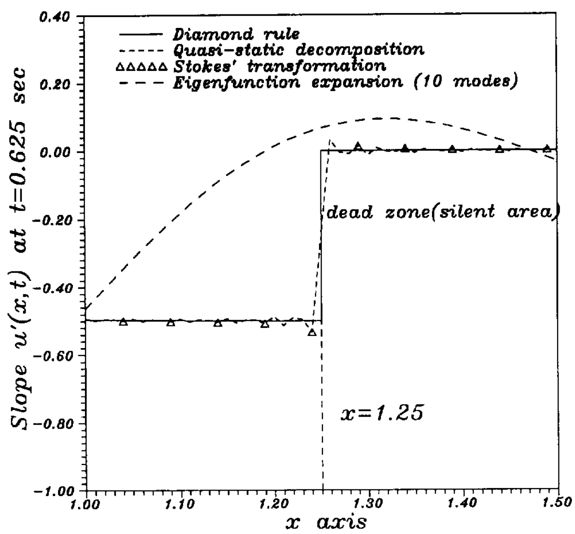

Fig. 4. Local slope profile near $x = 1{\cdot}25$ m by quasi-static decomposition, Stokes' transformation, eigenfunction expansion and the diamond rule.

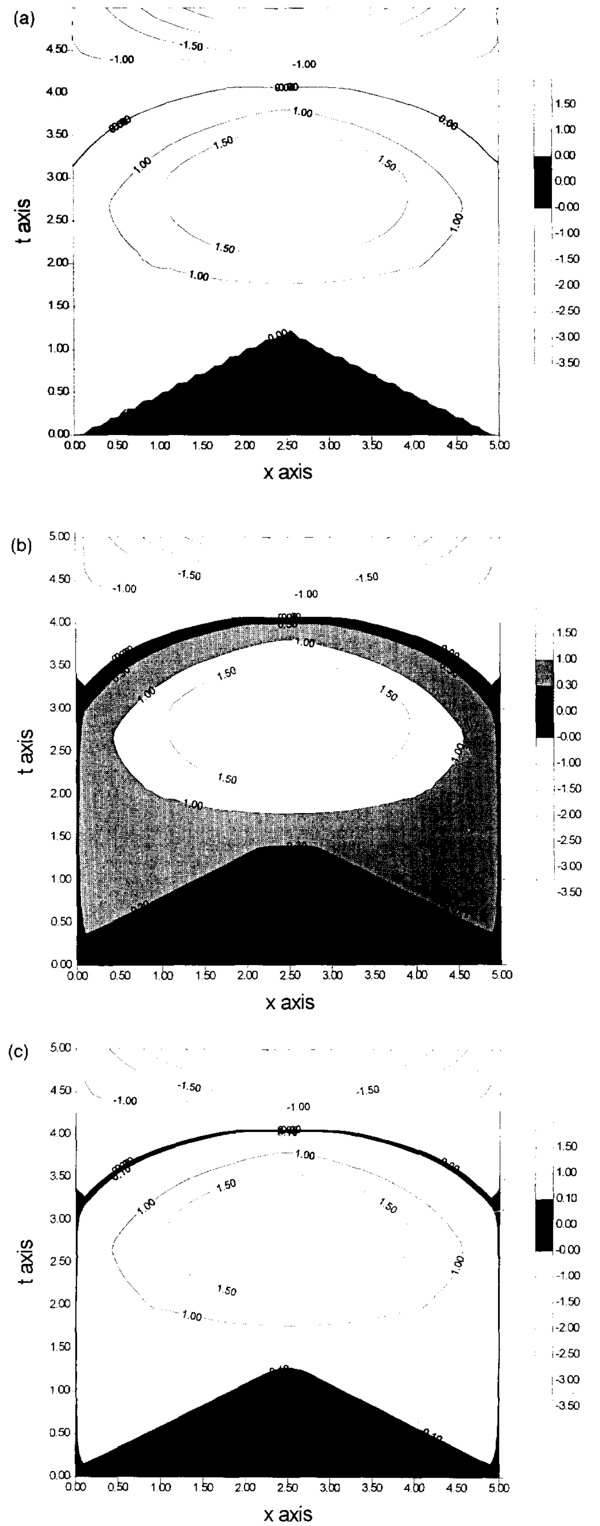

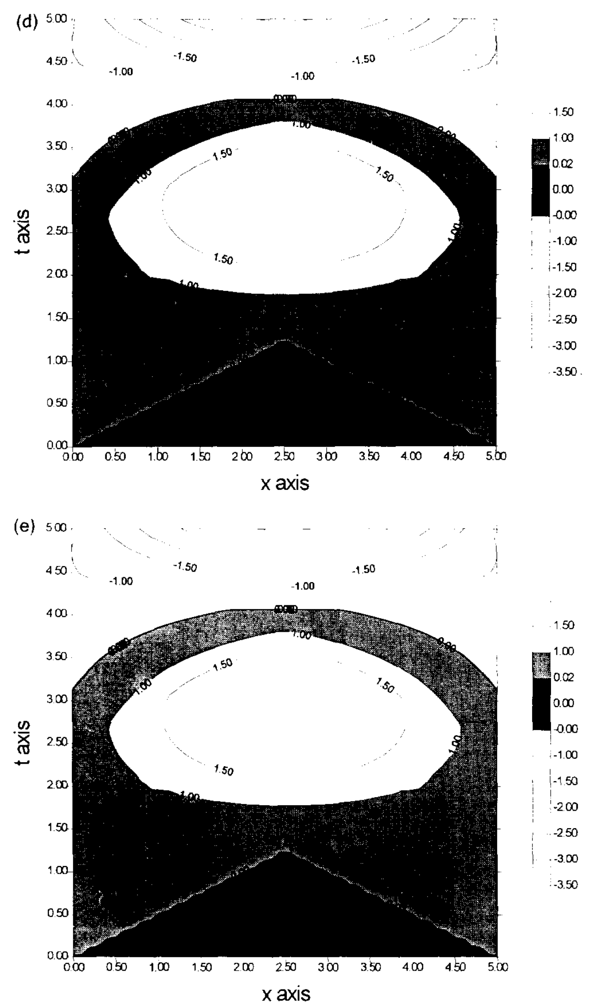

Fig. 5. Contour plot for $u(x,t)$ by (a) the diamond rule, (b) eigenfunction expansion, (c) eigenfunction expansion with Cesàro treatment, (d) the quasi-static decomposition method, and (e) Stokes' transformation.

5.4 Series solution regularized by the Stokes' transformation

By substituting l, c and $\sin(t)$ into eqns (84) and (85), we have

$$u(x,t) = \sin(t) + \sum_{n=1}^{\infty}\left(\frac{-2cl}{(c^2n^2\pi^2 - l^2)}\sin(n\pi ct/l) + \frac{2n\pi c^2}{(c^2n^2\pi^2 - l^2)}\sin(t) - \frac{2\sin(t)}{n\pi}\right)(1-(-1)^n)\sin(n\pi x/l) \quad (96)$$

$$u'(x,t) = \sum_{n=1}^{\infty}\left[\frac{-2cn\pi\sin(n\pi ct/l)}{(c^2n^2\pi^2 - l^2)}(1-(-1)^n) + \frac{2(n\pi c)^2\sin(t)}{l(c^2n^2\pi^2 - l^2)}(1-(-1)^n) + \frac{2\sin(t)}{l}((-1)^n - 1)\right]\cos(n\pi x/l) \quad (97)$$

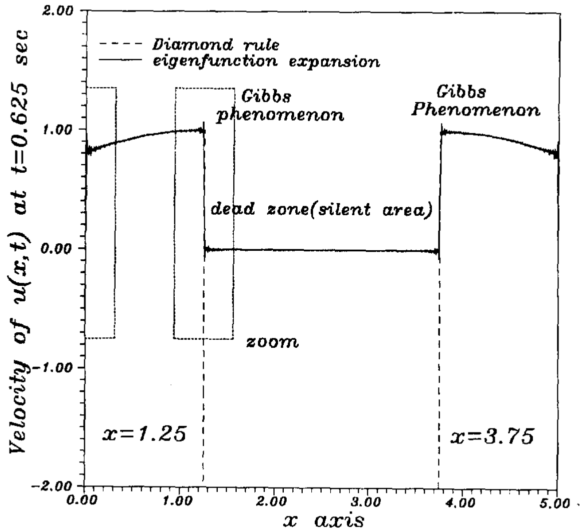

Fig. 6. Velocity profile by using quasi-static decomposition, Stokes' transformation and the diamond rule at $t = 0{\cdot}625$ s.

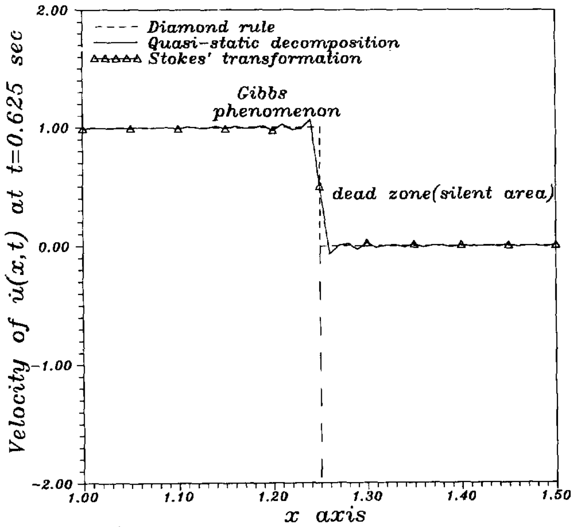

Fig. 8. Velocity profile by using eigenfunction expansion and the diamond rule at $t = 0{\cdot}625$ s.

$$u_t(x,t) = \cos(t) + \sum_{n=1}^{\infty}\left[\frac{-2n\pi c^2}{(c^2n^2\pi^2 - l^2)}\cos(n\pi ct/l) + \frac{2n\pi c^2}{(c^2n^2\pi^2 - l^2)}\cos(t) + \frac{-2}{n\pi}\cos(t)\right](1-(-1)^n)\sin(n\pi x/l). \quad (98)$$

5.5 Series solution by using the quasi-static decomposition method

By substituting l, c and $\sin(t)$ into eqns (86) and (87), we have

$$u(x,t) = \sin(t) + \sum_{n=1}^{\infty}\frac{-2l}{(c^2n^2\pi^2 - l^2)}(1-(-1)^n) \times (c sin(n\pi ct/l) - \frac{l}{n\pi}\sin(t))\sin(n\pi x/l) \quad (99)$$

$$u'(x,t) = \sum_{n=1}^{\infty}\frac{-2l}{(c^2n^2\pi^2 - l^2)}(1-(-1)^n)(c\sin(n\pi ct/l) - \frac{l}{n\pi}\sin(t))(n\pi/l)\cos(n\pi x/l). \quad (100)$$

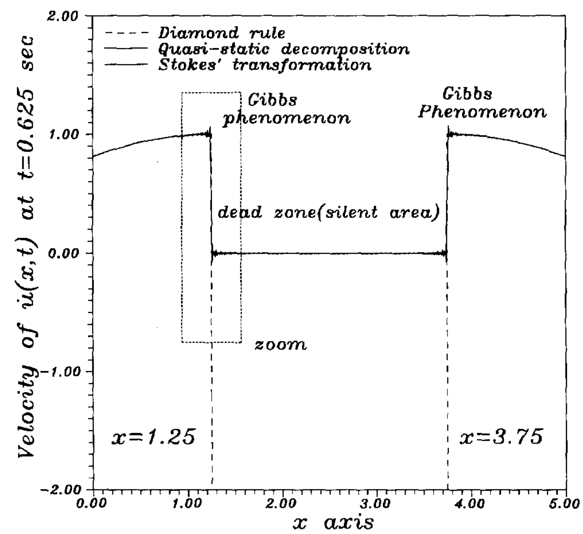

Fig. 7. Local velocity profile near $x = 1{\cdot}25$ m by using quasi-static decomposition, Stokes' transformation and the diamond rule.

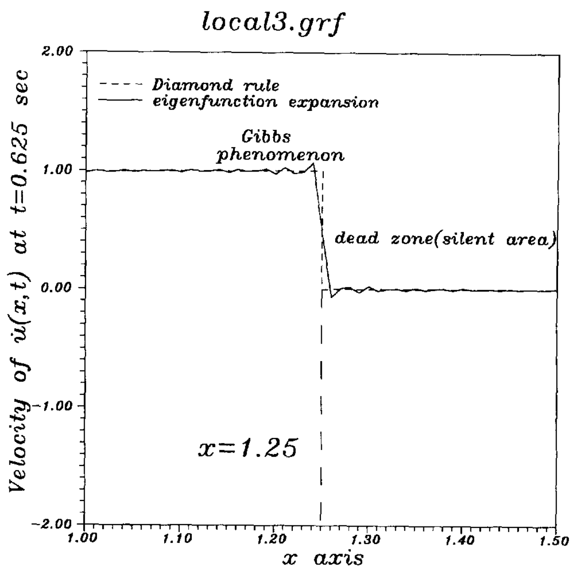

Fig. 9. Local velocity profile near $x = 1{\cdot}25$ m by using eigenfunction expansion and the diamond rule.

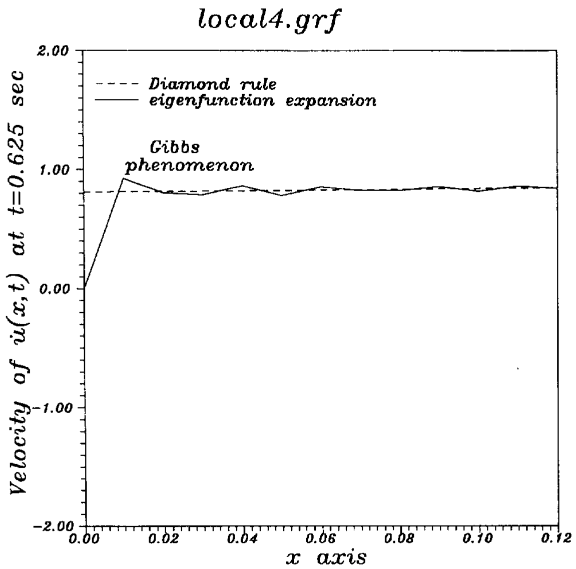

Fig. 10. Local velocity profile near $x = 0$ m by using eigenfunction expansion and the diamond rule.

It is interesting to find that eqn (96) for the series solution of the Stokes' transformation can be transformed into eqn (99) for the series solution in terms of the quasi-static decomposition method after using the asymptotic series expansion.

The displacement profiles at $t = 0{\cdot}625$ s, using the diamond rule, eigenfunction expansion, quasi-static decomposition and Stokes' transformation are shown in Fig. 2. A silent area, or so-called dead zone, from $x = 1{\cdot}25$ m to $x = 3{\cdot}75$ m is found to be zero displacement since the wave front has not arrived at this region yet. The eigenfunction expansion results in the Gibbs phenomenon near the boundaries $x = 0$ m and $x = 5$ m. The slope profiles at $t = 0{\cdot}625$ s using the diamond rule, eigenfunction expansion, quasi-static decomposition and Stokes' transformation are shown in Fig. 3. The eigenfunction expansion results in series divergence since term by term differentiation with respect to x is not permissible. After including the boundary terms by using Stokes' transformation, the series converges to the exact solution by using the diamond rule. The slopes are obtained by using the quasi-static decomposition method and the Stokes' transformation; both methods present the Gibbs phenomenon at $x = 1{\cdot}25$ m and $x = 3{\cdot}75$ m, where discontinuity occurs due to the interfaces between the silent area and unsilent area. Only the diamond rule can describe the discontinuity very well since the solution is separately described in each region. The zoom view of the local profile by using quasi-static decomposition, Stokes' transformation, eigenfunction expansion and the diamond rule are shown in Fig. 4 at $x = 1{\cdot}25$ m only since antisymmetry at $x = 3{\cdot}75$ m is known.

The contour plot for $u(x, t)$ by using (a) the diamond rule, (b) the eigenfunction expansion, (c) the Cesàro treatment, (d) the quasi-static decomposition method and (e) the Stokes' transformation are shown in Fig. 5(a)–(e), respectively. All of the five figures from (a) to (e) agree very well and show the same silent area in the shadow triangle. Figure 5(b) shows the Gibbs phenomenon of two boundary layers near $x = 0$ m and $x = 5$ m, which can be diminished by the Cesàro treatment as shown in Fig. 5(c). Figure 6 shows the velocity profile by using quasi-static decomposition, Stokes' transformation and the diamond rule at $t = 0{\cdot}625$ s. It is found that the Gibbs phenomenon is also present near $x = 1{\cdot}25$ m and $x = 3{\cdot}75$ m, where discontinuity occurs due to the interfaces between the silent area and unsilent area. Figure 7 shows the zoom view of the local velocity profile near $x = 1{\cdot}25$ m by using the quasi-static decomposition, Stokes' transformation and the diamond rule. Figure 8 shows the velocity profile by eigenfunction expansion and the diamond rule at $t = 0{\cdot}625$ s. The Gibbs phenomenon is found at four positions for eigenfunction expansion method, not only at the boundary points $x = 0$ m and $x = 5$ m, but also at the interface points $x = 1{\cdot}25$ and $3{\cdot}75$ m. Figure 9 shows the local velocity profile near $x = 1{\cdot}25$ m by using eigenfunction expansion method and the diamond rule. Figure 10 shows the local velocity profile near $x = 0$ m by using eigenfunction expansion and the diamond rule. Comparing Fig. 8 with Fig. 3, it is found that termwise differentiation with respect to time is permissible for the eigenfunction expansion method instead of series divergence for differentiation with respect to x in Fig. 3. The displacement profile in Fig. 2 and the velocity profile in Fig. 8 both present the Gibbs phenomenon at $x = 0$ and 5 m for eigenfunction expansion. In Fig. 6, the velocity profile presents the Gibbs phenomenon at $x = 1{\cdot}25$ and $3{\cdot}75$ m for both the quasi-static decomposition method and the Stokes' transformation method although the Gibbs phenomenon does not exist at the boundary points $x = 0$ and $x = l$.

6 CONCLUSIONS

The dual series representations for intial-boundary value problems of dynamic elasticity have been proposed, and a string example has demonstrated its validity. Dual series representation (DSR) can be seen as an extension of dual integral equations (DIE). The Cauchy principal value in DIE is transformed into the convergence in the mean for the Gibbs phenomenon in DSR, and the Hadamard principal value for dealing with the divergent integral in DIE is similar to using the Stokes' transformation to avoid the divergent series in DSR. Also, the regularization technique of Cesàro mean can extract the finite part. Available techniques have been compared with the proposed method, and the results are satisfactory. The method of Stokes' transformation is recommended not only because of its convergence rate, but also because it is free from determining the quasi-static solution. The technique has been successfully applied to flexural beam.[17]

REFERENCES

1. Hong, H.-K. & Chen, J. T., Exact solution of potential flow around a line pump and on supersingularity of normal derivative of double layer potential. *The Tenth National Conference on Theoretical and Applied Mechanics*, Kaohsiung,Taiwan, 1986, pp. 571–74 (in Chinese).
2. Chen, J. T., On Hadamard principal value and boundary integral formulation of fracture mechanics. Master Thesis, Institute of Applied Mechanics, National Taiwan University, 1986.
3. Hong, H.-K. & Chen, J. T., Derivation of integral equations in elasticity. *J. Eng. Mech. Div., ASCE*, 1988, **114**(6), Em5, 1028–44.
4. Chen, J. T. & Hong, H.-K., On the dual integral representation of boundary value problem in Laplace equation. *Boundary Elements Abstracts*, 1933, **4**(3), 114–16.
5. Chen, J. T. & Hong, H.-K., *Boundary Element Method.* 2nd Edn, New World Press, Taipei, Taiwan, 1992 (in Chinese).
6. Chen, J. T., Hong, H.-K. & Chyuan, S. W., Boundary element analysis and design in seepage flow problems with sheetpiles. *Finite Elements in Analysis and Design*, 1994, **17,** 1–20.
7. Chen, J. T. & Hong, H.-K., Dual boundary integral equations at a corner using contour approach around singularity. *Adv. Engng Software*, 1994, **21**(3), 169–78.
8. Portela, A., Aliabadi, M. H. & Rooke, D. P., The dual boundary element method: effective implementation for crack problems. *Int. J. Num. Meth. Engng*, 1992, **33,** 1269–87.
9. Leitao, V., Aliabadi, M. H. & Rooke, D. P., The dual boundary element formulation for elastoplastic fracture mechanics. *Int. J. Num. Meth. Engng*, 1995, **38,** 315–33.
10. Chen, W. H. & Chen, T. C., An efficient dual boundary element technique for a two-dimensional fracture problem with multiple cracks. *Int. J. Num. Meth. Engng*, 1995, **38,** 1739–56.
11. Mindlin, R. D. & Goodman, L. E., Beam vibrations with time-dependent boundary conditions. *J. Appl. Mech., ASME*, 1950, **17,** 377–80.
12. Chen, J. T., Hong, H.-K., Yeh, C. S. & Chyuan, S. W., Integral representations and regularizations for divergent series solution of a beam subjected to support motion. *Earthqu. Engng Struct. Dynamics*, 1996. To be published.
13. Hong, H.-K. & Chen, J. T., On the dual integral representation and its application to vibration problems. In *Stress Analysis, Boundary Elements XV*, Vol. 2, pp. 377–90, ed. Rénčis, J. J. & Brebbia, C. A. Computational Mechanics Publication, Southampton, 1993.
14. Chen, L. Y., Chen, J. T., Hong, H. K. & Chen, C. H., Application of Cesàro Mean and the L-curve for deconvolution problem. *Soil Dynam. Earthqu. Engng*, 1995, **14**(5), 361–73.
15. Krishnasamy, G., Rizzo, F. J. & Rudolphi, T. J., Hypersingular boundary integral equations: their occurrence, interpretation, regularization and computation. In *Developments in Boundary Element Methods*, Vol. 7, *Advanced Dynamic Analysis by Boundary Element Methods*, ed. P. K. Banerjee & S. Kobayashi. Elsevier Applied Science, London, 1992.
16. Chen, J. T., Hong, H.-K. & Yeh, C. S., Modal reaction method for modal participation factor of support motion problems. *Commun. Num. Meth. Engng*, 1995, **11**(6), 479–90.
17. Chen, J. T., Tsaur, D. H. & Hong, H.-K., An alternative method for transient and random responses of structures subjected to support motions. *Engineering Structures*, 1997. To be published.